

## Analysis of magnetotransport data of $Tl_2Mn_2O_7$ pyrochlore: evidence for half-metallicity

This article has been downloaded from IOPscience. Please scroll down to see the full text article.

2004 J. Phys.: Condens. Matter 16 8725

(<http://iopscience.iop.org/0953-8984/16/47/022>)

View [the table of contents for this issue](#), or go to the [journal homepage](#) for more

Download details:

IP Address: 129.252.86.83

The article was downloaded on 27/05/2010 at 19:13

Please note that [terms and conditions apply](#).

# Analysis of magnetotransport data of $\text{Tl}_2\text{Mn}_2\text{O}_7$ pyrochlore: evidence for half-metallicity

P Velasco, J A Alonso<sup>1</sup>, M T Casais, M J Martínez-Lope and J L Martínez

Instituto de Ciencia de Materiales de Madrid (CSIC), Cantoblanco, 28049, Madrid, Spain

E-mail: ja.alonso@icmm.csic.es

Received 21 September 2004, in final form 20 October 2004

Published 12 November 2004

Online at [stacks.iop.org/JPhysCM/16/8725](http://stacks.iop.org/JPhysCM/16/8725)

doi:10.1088/0953-8984/16/47/022

## Abstract

Theoretical calculations have suggested that the  $\text{Tl}_2\text{Mn}_2\text{O}_7$  pyrochlore, exhibiting colossal magnetoresistance (CMR) properties, is a half-metal. However, no direct evidence for the half-metallicity had been described to date. In this paper we report on the results of an in-depth study of the transport and magnetotransport properties of this material, revealing that only the minority band conduction electrons contribute to the charge transport.

(Some figures in this article are in colour only in the electronic version)

## 1. Introduction

In recent years, materials exhibiting colossal magnetoresistance (CMR) properties have attracted a lot of attention [1], due to their potential use as magnetic sensors. The study of the CMR oxides was initiated in the hole-doped  $\text{RMnO}_3$  ( $\text{R}$  = rare-earth) perovskites, showing ferromagnetic and metallic behaviour below the Curie temperature ( $T_C$ ). Then, CMR properties were also reported in several non-perovskite oxides ( $\text{Tl}_2\text{Mn}_2\text{O}_7$ ,  $\text{CrO}_2$ ,  $\text{Fe}_3\text{O}_4$ ). Among them,  $\text{CrO}_2$  and  $\text{Tl}_2\text{Mn}_2\text{O}_7$  have been much less studied due to the difficulties inherent to their high-pressure preparation.

$\text{Tl}_2\text{Mn}_2\text{O}_7$  pyrochlore has been studied by several groups [2–8]. Several substituted families [3, 9–17] have also been described. Previously reported data [2–8] indicate that  $\text{Tl}_2\text{Mn}_2\text{O}_7$  is a ferromagnetic (FM) material, with a transition temperature around 120 K. This magnetic transition is concomitant with a metal-to-insulator (MI) transition, with the metallic behaviour in the FM region and the insulator behaviour in the paramagnetic (PM) region. Therefore, for this compound transport and magnetism are strongly correlated.

The mechanism responsible for the magnetism in  $\text{Tl}_2\text{Mn}_2\text{O}_7$  and derivative compounds can be considered to be a superposition of two processes [18]: a conventional Mn–O–Mn

<sup>1</sup> Author to whom any correspondence should be addressed.

superexchange (SE) and an indirect exchange (IE) due to the hybridization of the Tl–O' conduction band with the Mn band. These two mechanisms also explain the intimate correlation observed between magnetism and transport. CMR properties are driven, therefore, by the suppression of the magnetic fluctuations near  $T_C$  when an external magnetic field is applied, strongly reducing the magnetic scattering [6, 9, 19].

Band structure calculations [20] reveal that  $\text{Tl}_2\text{Mn}_2\text{O}_7$  is a half-metallic compound. In a half-metal (different from a semi-metal) there is a spin-differentiated density of states (DOS) [21, 22]. That is, there is a difference between the majority (spin up) and the minority (spin down) DOS. But the essential characteristic of a half-metal is that only one of the channels contributes to the electronic transport. In the case of  $\text{Tl}_2\text{Mn}_2\text{O}_7$ , the only carriers that take part in the transport are the minority electrons, coming from the hybridization of the Tl(6s)/O'(2p) band with the Mn( $t_{2g}$ ) bands. The majority holes, coming from the Mn( $t_{2g}$ )/O(2p) bands, are very heavy and do not participate in the transport process.

However, to date no experimental evidence for the half-metallicity of  $\text{Tl}_2\text{Mn}_2\text{O}_7$  has been reported. In the present study we report on the analysis of transport data that reveals the half-metallic character of this pyrochlore.

## 2. Experimental details

$\text{Tl}_2\text{Mn}_2\text{O}_7$  was prepared as a polycrystalline material by solid-state reaction under high-pressure and high-temperature conditions, as reported elsewhere [13, 23]. The previously described structural characterization [23] determined that  $\text{Tl}_2\text{Mn}_2\text{O}_7$  crystallizes in a conventional pyrochlore cubic structure, with a lattice parameter  $a_0 \cong 9.90 \text{ \AA}$ . Neutron powder diffraction data showed occupation factors for Tl and O' positions slightly lower than unity, revealing a small deficiency in the Tl and oxygen contents in the present sample. Therefore, the crystallographic formula can be written as  $\text{Tl}_{1.944(6)}\text{Mn}_2\text{O}_{6.96(1)}$  [23].

Transport and magnetotransport measurements have been carried out in a Physical Properties Measurement System (PPMS) cryostat, from Quantum Design, in compact pellets of dimensions about  $5 \times 3 \times 2 \text{ mm}^3$ . A conventional four-point arrangement was adopted for the resistivity measurements, while for the Hall-effect measurements a five-point configuration was used [24]. Temperatures ranged from 2 to 380 K, and magnetic fields up to 9 T.

## 3. Results

The variation of the electrical resistivity with temperature is plotted on the right-hand axis of figure 1(a). We represent the measurement without magnetic field in solid squares, and in solid circles the measurement under a magnetic field of 9 T. Observe that the MI transition is concomitant with the magnetic transition: the susceptibility is given on the left-hand axis. When we apply an external magnetic field, the resistivity drops, and the MI transition shifts to higher temperatures. This dependence of the resistivity on the magnetic field is known as magnetoresistance (MR). In figure 1(b) we plot the temperature dependence of the MR ratio, defined as  $\text{MR}(H)(\%) = 100 \times [\rho(H) - \rho(0)]/\rho(0)$ . The maximum in the (negative) MR is displayed slightly above  $T_C$ , at about 130 K.

The dependence of the resistivity on the magnetic field is illustrated in figure 2. The resistivity for each temperature has been normalized to its value at zero field ( $\rho_0$ ). It is useful to compare all the curves in the same graph. This gives an idea of the magnitude of the change in the resistivity upon the application of a magnetic field. One can distinguish two different behaviours. For temperatures below and about  $T_C$  (top panel), the low-field variation is mainly linear with  $H$ ; and the variation rate decreases for higher fields, even reaching saturation for the 5 K resistivity. On the other hand, for temperatures above  $T_C$  (bottom panel) the variation

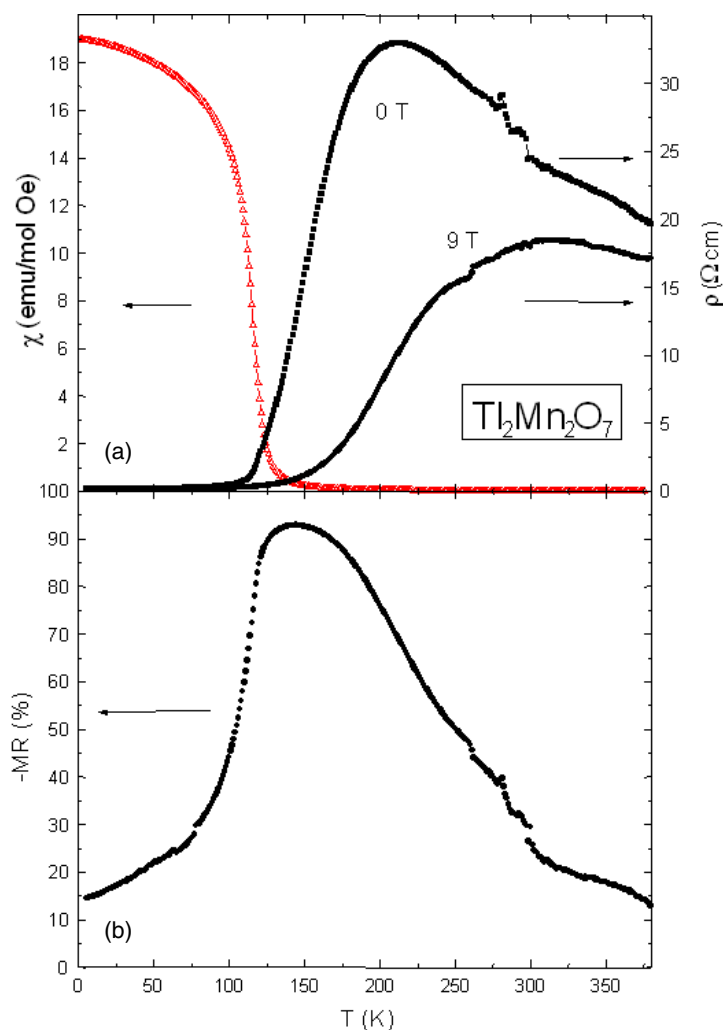


**Figure 1.** (a) Variation of the resistivity (right axis) and the magnetic susceptibility (left axis) with temperature. The resistivity was measured under no magnetic field ('0 T', squares) or under a magnetic field of 9 Tesla ('9 T', circles). A drop in resistivity is observed when reaching the ferromagnetic phase. (b) Variation with temperature of the magnetoresistance ratio. For a definition of the magnetoresistance ratio see the text.

is almost quadratic, changing the curvature for very high fields (200 K) or not changing it at all (250 and 300 K). This indicates that the mechanism of the variation of the resistivity with the magnetic field is different whether we are in the FM region or in the PM region.

In order to find the density of carriers in the material, we performed a series of Hall effect measurements. We measured the Hall resistivity versus the magnetic field for different temperatures, above, below and at the transition. In figure 3 we show the variation of the transverse (Hall) resistivity with the applied field for the lowest temperatures. The slope is always negative, indicating that the carriers are, in the whole temperature range, electrons. The increase in the absolute value of the slope means that the number of carriers is decreasing as the temperature increases.

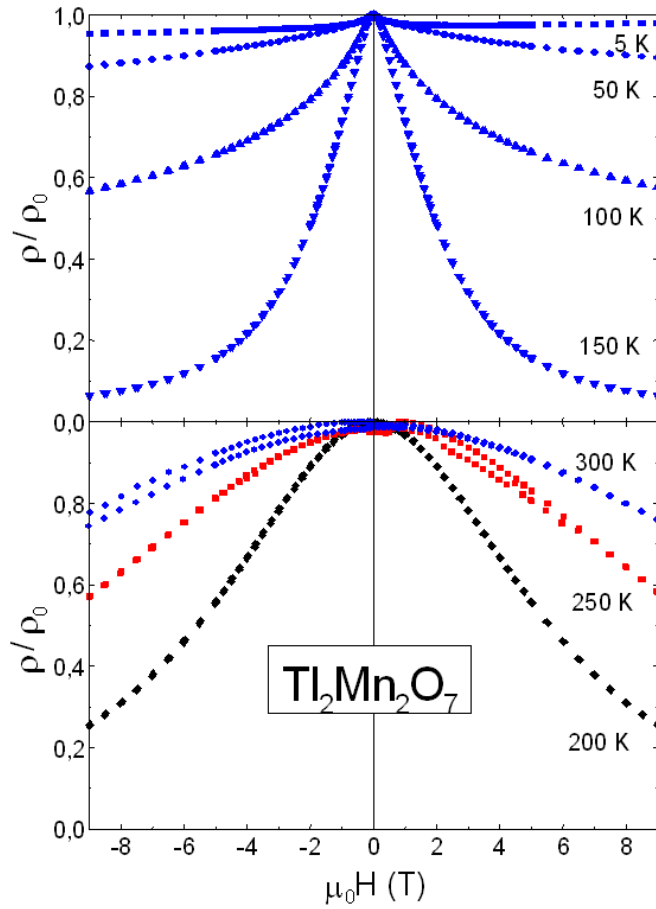


**Figure 2.** Dependence of the normalized resistivity on the magnetic field, at the indicated temperatures. Two different curvatures are observed either at low (upper panel) or high (lower panel) temperatures.

## 4. Analysis and discussion

### 4.1. Low-temperature resistivity

For the low-temperature resistivity, we fitted the data to the equation  $\rho = \rho_0 + AT^2e^{-\Delta_g/T}$ , and we found a very good agreement for temperatures up to 80 K (figure 4). The  $T^2$  dependence could indicate [25] either electron–electron or electron–magnon interactions. For the latter, the exponential factor would suggest a gap in the dispersion relation for magnons. But, from neutron scattering data [26] this gap is found to be  $\Delta < 0.04$  meV; that is,  $\text{Tl}_2\text{Mn}_2\text{O}_7$  has a gapless dispersion relation. Therefore, the  $T^2$  term is not due to electron–magnon interactions, but to electron–electron ones. In that case, the square dependence on temperature is related to spin-flip processes. Consequently, the exponential factor is associated with the *inaccessibility of majority spin states for spin-flip scattering processes*. This analysis evidences the half-metallicity of  $\text{Tl}_2\text{Mn}_2\text{O}_7$ . The value found for the gap,  $\Delta_g = 4.3(4)$  K =  $0.37(3)$  meV, is smaller than the Fermi energy at low temperatures ( $\varepsilon_F(5 \text{ K}) = 3.60$  meV, see below). This means that the Fermi level is close to the bottom of the majority conduction band.

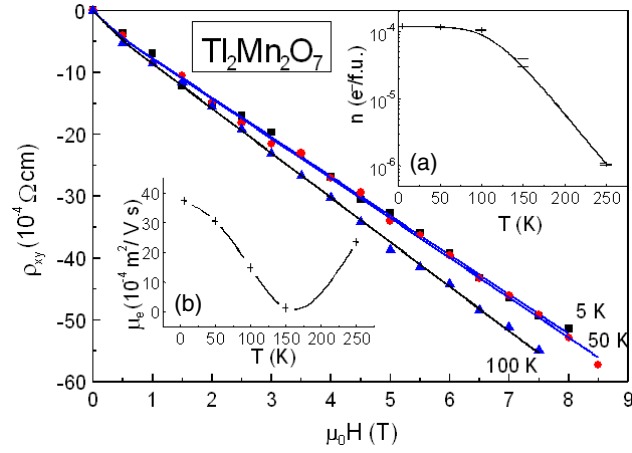


**Figure 3.** Thermal variation of the transverse resistivity (Hall effect), for temperatures below  $T_C$  (squares, 5 K; circles, 50 K; triangles, 100 K). The lines are fittings considering the anomalous Hall contribution (equation (3)). Insets: variation with temperature of (a) the density of electrons per formula unit, and (b) the mobility of those electrons. The curves are guides for the eye.

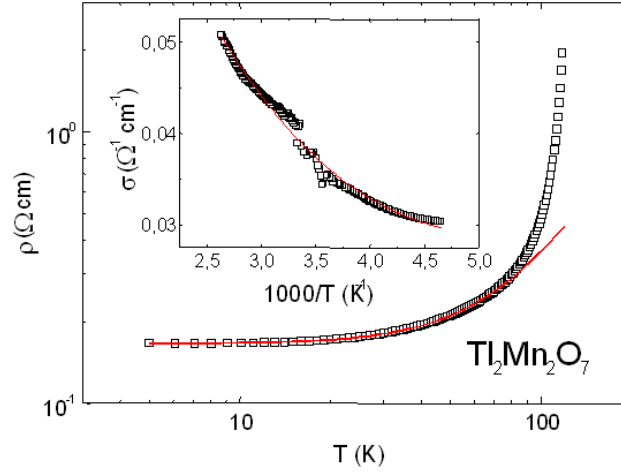


**Figure 4.** Log-log plot of the low-temperature resistivity of the  $\text{Tl}_2\text{Mn}_2\text{O}_7$  pyrochlore. Experimental data are represented by open squares. The curve corresponds to the fit to the function  $\rho = \rho_0 + AT^2 e^{-\Delta_g/T}$ . Inset: conductivity of the  $\text{Tl}_2\text{Mn}_2\text{O}_7$  pyrochlore versus the inverse of the temperature, for temperatures higher than 215 K. The curves represent the fit to an activated behaviour, according to equation (2).

#### 4.2. High-temperature resistivity

The electronic transport in the paramagnetic region is expected to have an important contribution from the polarons present in the material. The contribution to the conductivity via polaron hopping [16] is given by the equation [27]

$$\sigma_{\text{pol}} = \frac{1}{\rho_{\text{pol}}} = \sigma_0 \exp\left(-\frac{E_\sigma}{k_B T}\right) \quad (1)$$

**Table 1.** Hall coefficients and number of carriers for the  $\text{Tl}_2\text{Mn}_2\text{O}_7$  pyrochlore, at different temperatures.

$T$ (K)	$R_0$ ( $\text{cm}^3 \text{C}^{-1}$ )	$R_S$ ( $\text{cm}^3 \text{C}^{-1}$ )	$n$ ( $10^{-4} \text{e}^-/\text{fu}$ )
5	-6.36(7)	-2.7(7)	1.193(14)
50	-6.42(6)	-3.2(7)	1.181(12)
100	-7.16(7)	-4.4(9)	1.060(10)
150	-22(3)	—	0.35(5)
250	-723(15)	—	0.0105(2)

where  $\sigma_0 = g_d e^2 \nu_0 \delta / a k_B T$ . The factor  $g_d$  is determined by hopping geometry;  $\nu_0$  and  $a$  are the attempt frequency and hopping distance, respectively, and  $\delta$  is the carrier concentration per Mn site. A second contribution to the conductivity ( $\sigma_{\text{met}}$ ) arises from the metallic conductivity of the electrons, interacting with the lattice. Consequently, its form will be  $\sigma_{\text{met}} = A_{\text{met}}/T$ , with  $A_{\text{met}}$  not depending on  $T$ . The total conductivity can be written as

$$\sigma = \frac{1}{\rho} = \sigma_{\text{met}} + \sigma_{\text{pol}} = \frac{A_{\text{met}}}{T} + \frac{A_{\text{pol}}}{T} \exp\left(-\frac{E_\sigma}{k_B T}\right). \quad (2)$$

The resistivity data are well described by this equation, as shown in the inset of figure 4. The goodness of the fit indicates the presence and main role of the polarons in this system. The parameters of the fit are 4.31(12) and 197(8)  $\text{K} \Omega^{-1} \text{cm}^{-1}$  for  $A_{\text{met}}$  and  $A_{\text{pol}}$ , respectively; and  $E_\sigma$  is 85.0(16) meV. Since  $A_{\text{pol}} = g_d e^2 \nu_0 \delta / a k_B$ , from the fit parameters we can estimate the value of the density of carriers,  $\delta$ . For that estimation we took the hopping distance,  $a$ , as  $1 \text{ \AA} = 10^{-10} \text{ m}$ ; the geometric factor,  $g_d$ , of the order of unity, and for the attempt frequency a typical value of  $10^{13} \text{ s}^{-1}$ . Using those values, the density of carriers is of the order of  $10^{-4}$  carriers per Mn site. This value is really close to that experimentally found by Hall effect measurements as described below.

### 4.3. Hall effect

In an FM metal there are two contributions to the Hall effect: a ‘normal’ one, coming from the interactions of the conduction electrons with the magnetic field, and an ‘anomalous’ one, coming from the interaction with the magnetization [28]. Therefore, the transverse (Hall) resistivity is usually written in the form

$$\rho_{xy} = R_0 B + \mu_0 R_S M \quad (3)$$

where  $R_0$  and  $R_S$  are the ‘normal’ and ‘anomalous’ Hall coefficients, respectively;  $B$  is the magnetic induction and  $M$  the (macroscopic) magnetization. Consequently, we fitted the Hall-effect curves to that equation (figure 3), finding the Hall coefficients given in table 1. For high temperatures, as both  $B$  and  $M$  are linear with the field, it is not feasible to separate both contributions. Besides, as the (longitudinal) resistivity has increased (with respect to the low-temperature metallic region), it is more difficult to measure the transverse resistivity. For all these reasons, we take, above  $T_C$ ,  $\rho_{xy} = R_0 B$ . As for those temperatures  $\mu_0 M \ll B$ , the approximation is widely accepted (see, for instance, [29]).

From the ‘normal’ Hall coefficient, the density of carriers ( $n$ ) can be calculated, as  $R_0 = 1/ne$ , with  $e$  the electron charge. The values obtained for  $n$  are also given in table 1. Note that the number of carriers decreases with increasing temperature. For  $T < T_C$  the decrease is very small, but for temperatures above  $T_C$  there is a two-order-of-magnitude decrease (figure 3, inset (a)), explaining the resistivity peak. This reproduces the variation of the number of carriers with temperature from [29].

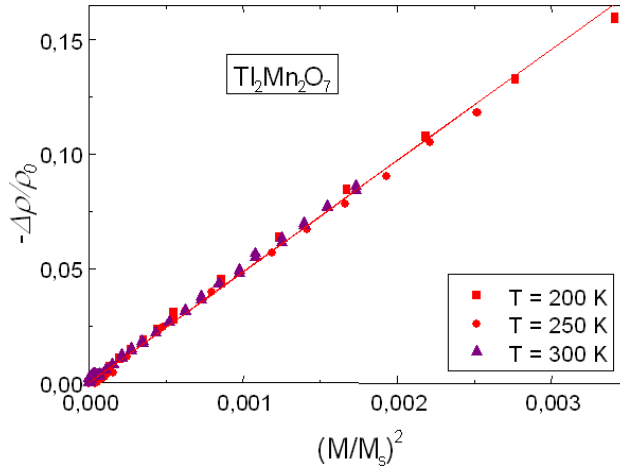


**Figure 5.** Magnetoresistance versus the square of the normalized magnetization for three different temperatures above the transition. See the linear scaling (solid line), and its temperature independence, in agreement with the Majumdar–Littlewood model.

#### 4.4. Majumdar–Littlewood model

Following the Majumdar–Littlewood model [6, 19], in a FM material with a low density of carriers the transport in the region above  $T_C$  will be limited by the scattering from magnetic fluctuations. Then, the magnetoresistance for those temperatures scales with the square of the magnetization, according to the equation  $\Delta\rho/\rho_0 = C(m/m_{\text{sat}})^2$ . In figure 5 we have plotted the magnetoresistance as a function of the square of the normalized magnetization. As predicted by the model, the dependence is linear and the scaling constant ( $C = 48.62(19)$ ) is temperature independent.

In the Majumdar–Littlewood model the authors distinguish between two different situations, depending on the value of the product  $k_F\xi$ , where  $k_F$  is the electron Fermi wavevector and  $\xi$  is the magnetic correlation length. From neutron scattering data, Lynn *et al* found  $\xi \sim 10 \text{ \AA}$  above  $T_C$  [26]. Besides, we found, for 250 K,  $k_F = 6.35 \times 10^7 \text{ m}^{-1}$ . That makes  $k_F\xi \sim 6 \times 10^{-2} \ll 1$ . Therefore, as they propose, we are in the region in which the conduction electrons will be self-trapped in small magnetic polarons. As the Bohr approximation is not valid in this region, the  $C \sim n^{-2/3}$  relation proposed by Majumdar and Littlewood would not be valid in  $\text{Tl}_2\text{Mn}_2\text{O}_7$ .

## 5. Conclusions

The  $\text{Tl}_2\text{Mn}_2\text{O}_7$  pyrochlore has been found to be a ferromagnetic half-metal: in the density of states a gap between the majority and minority bands has been found by resistivity measurements, and the comparison of the density of states at the Fermi level obtained from Hall effect and specific heat reveals a large number of carriers in one of the bands (majority) not contributing to the transport.

$\text{Tl}_2\text{Mn}_2\text{O}_7$  presents a very low density of states at the Fermi level, as theoretically predicted. There is a clear correlation between transport and magnetism: parallel alignment of the magnetic moments favours the carriers' mobility. We have found the existence of magnetic polarons for temperatures above  $\sim 1.2 T_C$ . Activated polaron-hopping plays an important role in the high temperature transport. Both the reduction in the number of carriers and a decrease in their mobility are responsible for the metal–insulator transition found around  $T_C$ .



## Acknowledgments

We acknowledge the financial support of the Spanish Ministerio de Ciencia y Tecnología for projects MAT2004-0479 and MAT2002-1329. We thank Professor J M D Coey for helpful discussion.

## References

- [1] Rao C N R and Raveau B (ed) 1998 *Colossal Magnetoresistance and Other Related Properties in 3d Oxides* (Singapore: World Scientific)
- [2] Shimikawa Y, Kubo Y and Manako T 1996 *Nature* **379** 53
- [3] Cheong S-W, Hwang H Y, Batlogg B and Rupp L W 1996 *Solid State Commun.* **98** 163
- [4] Subramanian M A, Toby B H, Ramirez A P, Marshall W J, Sleight A W and Kwei G H 1996 *Science* **273** 81
- [5] Kwei G H, Booth C H, Bridges F and Subramanian M A 1997 *Phys. Rev. B* **55** R688
- [6] Majumdar P and Littlewood P B 1998 *Nature* **395** 479
- [7] Sushko Yu V, Kubo Y, Shimakawa Y and Manako T 1999 *Physica B* **259–261** 831
- [8] Zhao J H, Kunkel H P, Zhou X Z, Williams G and Subramanian M A 1999 *Phys. Rev. Lett.* **83** 219
- [9] Ramirez A P and Subramanian M A 1997 *Science* **277** 546
- [10] Martínez B, Senis R, Foncuberta J, Obradors X, Cheihk-Rouhou W, Strobel P, Bougerol-Chaillout C and Pernet M 1999 *Phys. Rev. Lett.* **83** 2022
- [11] Senis R 2000 Propiedades magnéticas y de transporte en óxidos de manganeso con magnetorresistencia colosal:  $\text{La}_{1-x}\text{Sr}_x\text{MnO}_3$ ,  $\text{Tl}_2\text{Mn}_{2-x}\text{Ru}_x\text{O}_7$  *PhD Thesis* Universitat Autònoma de Barcelona and Université Joseph Fourier
- [12] Cheihk-Rouhou W, Senis R, Chaillout C, Strobel P, Martínez B and Obradors X 1999 *Mater. Res. Soc. Symp. Proc.* **547** 27
- [13] Alonso J A, Martínez J L, Martínez-Lope M J, Casais M T and Fernández-Díaz M T 1999 *Phys. Rev. Lett.* **82** 189
- [14] Velasco P, Alonso J A, Casais M T, Martínez-Lope M J, Martínez J L and Fernández-Díaz M T 2002 *Phys. Rev. B* **66** 174408
- [15] Alonso J A, Martínez-Lope M J, Casais M T, Velasco P, Martínez J L, Fernández-Díaz M T and de Paoli J M 1999 *Phys. Rev. B* **60** R15024
- [16] Velasco P, Alonso J A, Martínez-Lope M J, Casais M T, Martínez J L, Fernández-Díaz M T and De Paoli J M 2001 *Phys. Rev. B* **64** 184436
- [17] Velasco P, Alonso J A, Martínez-Lope M J, Casais M T, Martínez J L, Fernández-Díaz M T and de Paoli J M 2001 *J. Phys.: Condens. Matter* **13** 10991
- [18] Núñez-Regueiro M D and Lacroix C 2001 *Phys. Rev. B* **63** 14417
- [19] Majumdar P and Littlewood P 1998 *Phys. Rev. Lett.* **81** 1314
- [20] Singh D J 1997 *Phys. Rev. B* **55** 313
- [21] Coey J M D and Venkatesan M 2002 *J. Appl. Phys.* **91** 8345
- [22] Pickett W E and Moodera J S 2001 *Phys. Today* (May) 39
- [23] Alonso J A, Martínez-Lope M J, Casais M T, Martínez J L and Fernández-Díaz M T 2000 *Chem. Mater.* **12** 1127
- [24] Velasco P 2002 Synthesis and characterization of new  $\text{Tl}_2\text{Mn}_2\text{O}_7$ -related pyrochlores with colossal magnetoresistance *PhD Thesis* Universidad Autónoma de Madrid
- [25] Watts S M, Wirth S, von Molnár S, Barry A and Coey J M D 2000 *Phys. Rev. B* **61** 9621
- [26] Lynn J W, Vasiliu-Doloc L and Subramanian M A 1998 *Phys. Rev. Lett.* **80** 4582
- [27] Chun S H, Salamon M B, Tomioka Y and Tokura Y 2000 *Phys. Rev. B* **61** R9225
- [28] Berger L and Bergmann G 1980 *The Hall Effect and its Applications; Proc. Commemorative Symp. on the Hall Effect and its Applications (The Johns Hopkins University, Baltimore, Maryland, Nov. 1979)* (New York: Plenum) pp 55–76 chapter (The Hall Effect of Ferromagnets)
- [29] Imai H, Shimakawa Y, Sushko Y V and Kubo Y 2000 *Phys. Rev. B* **62** 12190